Aeolian Research 28 (2017) 39–49

Contents lists available at ScienceDirect

Aeolian Research

journal homepage: www.elsevier.com/locate/aeolia

Wind sorting affects differently the organo-mineral composition of saltating and particulate materials in contrasting texture agricultural soils

Laura Antonela Iturri [a,b], Roger Funk [c], Martin Leue [c], Michael Sommer [c], Daniel Eduardo Buschiazzo [a,b,d,*]

[a] Institute for Earth and Environmental Sciences of La Pampa, National Council for Research and Technology (INCITAP, CONICET-UNLPam), cc 186, 6300 Santa Rosa, Argentina
[b] National University of La Pampa (UNLPam), cc 300, 6300 Santa Rosa, Argentina
[c] Institute of Soil Landscape Research, Leibniz Centre for Agricultural Landscape Research (ZALF), 15374 Müncheberg, Germany
[d] National Institute for Agricultural Technology (INTA), Anguil Experimental Station, 6326 Anguil, Argentina

ARTICLE INFO

Article history:
Received 1 April 2017
Revised 17 July 2017
Accepted 17 July 2017

Keywords:
Wind erosion
Dust
Granulometry
Soil organic carbon

ABSTRACT

There is little information about the mineral and organic composition of sediments eroded by wind at different heights. Because of that, wind tunnel simulations were performed on four agricultural loess soils of different granulometry and their saltating materials collected at different heights. The particulate matter with an aerodynamic diameter mainly smaller than 10 μm (PM10) of these soils was obtained separately by a laboratory method. Results indicated that the granulometric composition of sediments collected at different heights was more homogeneous in fine- than in sandy-textured soils, which were more affected by sorting effects during wind erosion. This agrees with the preferential transport of quartz at low heights and of clay minerals at greater heights. SOC contents increased with height, but the composition of the organic materials was different: stable carboxylic acids, aldehydes, amides and aromatics were preferentially transported close to the ground because their were found in larger aggregates, while plant debris and polysaccharides, carbohydrates and derivatives of microbial origin from organic matter dominated at greater heights for all soil types. The amount of SOC in the PM10 fraction was higher when it was emitted from sandy than from fine textured soils. Because of the sorting process produced by wind erosion, the stable organic matter compounds will be transported at low heights and local scales, modifying soil fertility due to nutrient exportation, while less stable organic compounds will be part of the suspension losses, which are known to affect some processes at regional- or global scale.

1. Introduction

Wind erosion (WE) is one of the most important processes in soils of arid and semi-arid environments in the world, both for soil formation and soil degradation. WE affects not only the soils but also other ecosystems far away due to the transport of particulate matter. Particles with a diameter less than 10 μm (PM10) are distributed in the atmosphere, and can stay suspended in the air for a long time. Thus, they affect directly the solar and terrestrial radiation, and cloud formation processes (Conen and Leifeld, 2014; Steinke et al., 2016). Other effects include carbon and nutrient losses at the erosion site and the addition of these materials in either adjacent or distant ecosystems, as well as the iron- and silica fertilization of the oceans (Harrison et al., 1997; Lal, 2003; Martin et al., 1991). Dust emissions also affect society by declining air quality and reducing visibility on roads trigger traffic accidents. Particles of the PM10 fraction, which can be inhaled, influence human health by causing lung diseases and early deaths (Dockery et al., 1993; Pope and Dockery, 2006). On agricultural lands, WE is a soil degrading process that removes predominantly particles of silt and clay and, due to its lower density, the soil organic matter (SOM) (Chappell, 2016; Nerger et al., 2017).

Information about the amount of soil that has been eroded is available for different climatic and land use conditions in the world, showing maximums of several hundreds of tons per hectare, per year (Schäfer et al., 1995; Funk, 1995; Michelena and Irurtia, 1995; Dong and Chen, 1997; Aimar, 2002; Hoffmann et al., 2011; Zobeck et al., 2013). However, the composition of the eroded material has been less studied, although some authors have found that the enrichment ratio (ER), i.e., the proportion between the concentration of a certain element in the eroded material and in the orig-

* Corresponding author at: Institute for Earth and Environmental Sciences of La Pampa, National Council for Research and Technology (INCITAP, CONICET-UNLPam), cc 186, 6300 Santa Rosa, Argentina.
E-mail address: debuschiazzo@yahoo.com (D.E. Buschiazzo).

http://dx.doi.org/10.1016/j.aeolia.2017.07.005
1875-9637/

inal soil, reaches values of 0.8 to 17, according to the element, the type of soil and the wind velocity (Funk, 1995; Aimar et al., 2002; Ravi et al., 2011; Sharratt et al., 2015; Webb et al., 2012).

WE is a transporting and sorting process resulting in two basic transport modes: the saltation and the suspension flux, which involve the transport of particles across low- and greater heights, respectively. Part of the suspension flux includes the PM10 fraction, which represents the most fertile components of a soil in the clay and fine silt sized fractions and degrades air quality when concentrations are elevated. The PM10 emissions in the Semiarid Central Region of Argentina (SCRA) are mainly caused by WE of agricultural soils, while in other parts of the world the sources are ephemeral lakes and deserts (Gaiero et al., 2004; Tanaka and Chiba, 2006; Lenes et al., 2012). In comparison to dust emissions from desert regions, dust from agricultural soils has special features such as a wider granulometric composition, large SOC content or biologically active components (Fröhlich-Nowoisky et al., 2012; Conen and Leifeld, 2014). Therefore, the SCRA is a suitable region for detailed studies of WE and dust emission processes as a function of the degradation rate or development status of the soils and land use intensity. Both, soil type and land use conditions will determine dust-releasing processes in this region as well as the composition of these materials.

In addition, the mineral and organic soil compounds, which are sorted by size or density during the erosion process, will result in different height distribution profiles. As soil dust from agricultural land is enriched in SOC compared to the original soil these losses will represent a disproportionate depletion of soil quality. Due to the low net primary production of most regions affected by WE, the removed nutrients and SOC can be regarded as an irretrievable loss at the landscape scale, these losses are not balanced (Buschiazzo and Funk, 2015; Goossens and Gross, 2002; Tan et al., 2011; Yan et al., 2005).

In the 1990s numerous measurement campaigns of WE were performed on experimental plots around the world, mainly focused on the quantification of soil loss. Nowadays the focus has changed to a more detailed and qualitative description of all aspects of wind-driven soil processes. This focus involves fine particles and SOC transportation as well as their influence on health, air quality and climate (Ajwa and Sullivan, 2011; Morman and Plumlee, 2013; Nordstrom and Hotta, 2004; Shao et al., 2011; Webb et al., 2016). The aim of this study is focused on analyzing the effect of the wind sorting process on both the mineral and organic composition of the particles transported at different heights from different texture agricultural soils.

2. Materials and methods

2.1. Soil sampling

Soil samples were taken randomly to a depth of 2.5 cm in a 100 m^2 area from four agricultural soils in the SCRA. The soils, covering a granulometric gradient, were two Typic Ustipsamments (TU-I and TU-II) and two Entic Haplustolls (EH-I and EH-II). EH-I and TU-I belong to experimental controlled plots located in Site I (Santa Rosa, Argentina) and EH-II and TU-II, to Site II (Anguil, Argentina). These soils are highly susceptible to WE due to their particle size composition and their relatively low SOM content. These soil characteristics are a product of the dry and windy environmental conditions, as well as management practices based on 70-year conventional tillage, no-irrigation and mixed rotation (wheat-sorghum-alfalfa), which frequently left the soil smooth and flat (Buschiazzo et al., 1998). Further information about the sampled sites is shown in Table 1.

2.2. Wind tunnel simulations

A push-type wind tunnel was used, which consisted of an axial fan driven by a Honda GX6 52 kW engine, a flow straightener and a measuring section of 6 m-length, 1 m-height and 0.5 m-width. More details of the wind tunnel and results of its calibration are published in Panebianco et al. (2016).

Soil samples were prepared for wind tunnel simulations by air drying and sieving through a 2 mm-mesh. The measurement section was filled with a 2.5 cm-thick layer of each soil and levelled to get a comparable grain roughness for all samples. Wind velocity was increased quickly, kept constant for four minutes and measured with a pressure anemometer at 0.05, 0.17, 0.315, 0.48 m-height above the surface. The vertical profile was obtained according to Eq. (1),

$$u_* = \frac{K(\mu_{Z_2} - \mu_{Z_1})}{\ln(Z_2 - Z_1)} \quad (1)$$

being, u_*, the friction velocity expressed in m s^{-1}; *K*, the von Karman constant (0.4); and u_{Z1} and u_{Z2}, the wind speed at heights Z_1 (0.05 m) and Z_2 (0.48 m). The measurement scheme allowed the calculation of the u_* (Roney and White, 2006). The free stream velocity was measured using a cup anemometer placed at the end of the wind tunnel, at a height of 0.7 m above the surface, out of the boundary layer.

Wind velocity and roughness resulted in an average u_* of 0.71 m s^{-1} (SD 0.10 and CV 14.27%). Simulations were performed in triplicate. The relatively short time of simulations resulted in stable conditions for the duration of the experiments, including wind velocity and horizontal mass flux or depletion of the original soil bed. The material mobilized by saltation during the wind tunnel simulations was collected with Big Spring Number Eight (BSNE) samplers (Fryrear et al., 1998) placed at heights of 0.05, 0.17, 0.315 and 0.48 m above the surface at the end of the wind tunnel. For further information about the experiments, see Avecilla et al. (2015).

2.3. Potential PM10 emission simulations

The particulate matter with a diameter predominantly smaller than 10 μm (PM10 fraction) was separated from each soil with a dust generator (Easy Dust Generator, EDG; Mendez et al., 2013) assembled with an electrostatic trap. This device simulates the

Table 1
Main characteristics of the studied soils.

Soil	Soil classification[1]	Location	Geographic location	Clay	Silt	Sand	Texture	SOC	pH
				%				% ± SD	
TU-I	Typic Ustipsamment	Santa Rosa	36° 33′ S 64° 18′ W	5	7	88	Sandy	1.12 ± 0.02	6.1
TU-II		Anguil	36° 34′ S 63° 59′ W	8	12	80	Loamy sand	0.97 ± 0.01	5.9
EH-I	Entic Haplustoll	Santa Rosa	36° 32′ S 64° 17′ W	10	19	71	Sandy loam	0.90 ± 0.03	6.7
EH-II		Anguil	36° 35′ S 63° 57′ W	17	36	47	Loam	1.04 ± 0.01	6.0

TU-I: Typic Ustipsamment from site I; TU-II: Typic Ustipsamment from site II; EH-I: Entic Haplustoll from site I; EH-II: Entic Haplustoll from Site II; SOC: soil organic carbon content; SD: standard deviation.

[1] Soil Survey Staff (1999).

PM10 emission process under laboratory controlled conditions using a rotary chamber.

Each soil sample used in the dust generator was previously sieved through a 2 mm-mesh and dried at 35 °C to avoid phyllosilicate denaturation. The duration of each run was between 20 and 30 min, until an amount of 0.5 to 1.0 g of the PM10 fraction was achieved. The collected material in the electrostatic trap was carefully removed with a non-electrostatic brush. After each run, the cover material of the dust-generating chamber and the brush were changed and all tools were completely cleaned to avoid any kind of cross-contamination.

2.4. Granulometry and carbon content

The bulk soils, the trapped sediments at the end of the wind tunnel and the PM10 fraction extracted from the soils with the laboratory method, were investigated for the following parameters:

1) granulometric composition of non-dispersed soil samples were placed in water, analyzed by a laser particle counter (Mastersizer 2000, Malvern Instruments). Particle fractions were classified as clay (0–3.9 μm), fine and medium silt (3.9–31 μm), coarse silt (31–62.5 μm), very fine sand (62.5–125 μm), fine sand (125–250 μm) and medium and coarse sand (250–2000 μm), according to Wentworth (1922).
2) total carbon content by dry combustion using an elemental analyzer (TruSpec CNS, LECO Instruments GmbH, DIN ISO 10694);

Moreover, in order to perform a characterization of the four studied bulk soils, their textural classification according to the USDA (Soil Survey Staff, 1999) was assessed, and the pH by potentiometry (1:2.5 soil: distilled water) (Mc Lean, 1982) was measured (Table 1).

Images of the 0.48 m-height trapped sediments were gained from scanning electron microscope (SEM, JEOL JSM6060 LV on SEI-mode) analyses. A laser-scanning microscope (Keyence VK – X100) was used to take images of the PM10 fractions.

2.5. Organo-mineral composition

The composition of the bulk soil, the trapped sediments and the PM10 fraction with respect to mineral (O—H of clay minerals and Si—O of quartz) and organic (aliphatic C—H, C=O and C=C and C—O-C of polysaccharides) functional groups was determined by Transmission Fourier-Transform Infrared Spectroscopy (transmission FTIR) in the mid-infrared range using a BIO-RAD FTS 135 spectrometer (BIO-RAD company, Cambridge, USA).

For transmission-FTIR analyses, 1 mg sample was mixed with 99 mg potassium bromide (3 sample replicates), finely ground in an agate mortar, and pressed into pellets. The transmission spectra were recorded as 16 co-added scans between wave number (WN) 4000 and 400 cm^{-1} at a resolution of 1 cm^{-1}, and corrected against ambient air as background. The spectra were converted to absorption units, smoothed (boxcar algorithm, factor 25), and corrected for baseline shifts using the software WIN-IR Pro 3.4 (Digilab, MA, USA). In the spectra, the signal intensities of both mineral and organic matter were analyzed using band assignments given in literature (Table A-1).

The signal intensities of the absorption bands were measured as heights from the total baseline with the exception of the C—H band intensities (WN 2956, 2925 and 2859 cm^{-1}), which were measured as the vertical distance from a local baseline plotted between tangential points to consider the effect of the broad O—H band at WN 3435 cm^{-1}. All FTIR signal intensities were normalized using the spectral area between WN 4000 and 400 cm^{-1}.

As free lime was not detected in the analyzed samples by means of FTIR spectroscopy, in agreement with soil pH values found, the total C contents belong only to organic compounds (SOC).

2.6. Statistical analysis

A simple ANOVA ($\alpha = 0.05$) was performed to test the differences in the granulometric composition, SOC contents and FTIR-signals between the bulk soils, the trapped sediments and the PM10 fraction within each soil and between soils, using Microsoft Excel/2016. The discriminant analyses between the FTIR spectra and the SOC values of 24 samples (bulk soils, trapped sediments and PM10 fractions) were made by a Partial Least Squares Regression (PLSR) using R, version 3.1.1 (R Core Team, 2014). Larger absolute loading values of signal intensities in certain WN regions imply a greater importance of these WN for the cumulated values of the respective principal components 1 or 2 displayed in the discriminant plot. The score plot of the most relevant components, 1 and 2 of the PLSR, were used to assess differences among the studied samples according to SOC content.

3. Results

3.1. Granulometry and SOC contents

The four studied soils were different in their granulometric composition and spanned the texture classes sandy to loamy. Their SOC contents were close to 1% (Table 1). The clay contents of non-dispersed samples of the trapped sediments at all saltation heights in the wind tunnel runs were not detectable or much lower compared to the bulk soils in the TU-I and EH-II. However, clay content was higher compared to the bulk soils at 0.05 and 0.48 m-height in the TU-II and at 0.05 m-height in the EH-II (Table 2).

This situation resulted in clay enrichment ratios (ER) of maximal 0.4 in those trapped sediments where clay was detected. However, the distribution of clay content with the height was different between soils: it was higher at lower heights in fine than in sandy textured soils (Table 2). Clay contents of the PM10 fraction were higher than in the bulk soil, shifting its ER to values between 1.3 and 3.2, being higher in fine than in sandy textured soils and significantly higher than the ER for clay of all the trapped sediments (0.1 to 0.4).

The ER for silt was close to 1 or slightly lower in all studied soils and saltation heights. Only the loamy sand TU-II showed ER ratios higher than 1 at the two greatest heights. The silt content was not detected or was much lower at smaller heights in the sandiest (TU-I) than in the finer textured soils (TU-II, EH-I and EH-II) (Table 2). The silt contents of the PM10 fraction were higher than in the bulk soil (Table 2), varying its ER from 9.7 to 2.1, being higher in sandy than in finer textured soils.

The very fine sand showed ER values higher than 1 in all studied soils and heights, varying between 1.1 and 2.1, with a tendency to increase with height in all soils. The very fine sand contents were lower at lower heights in the sandy soils than in the fine textured soils (Table 2). The ER of fine sand showed values between 1.2 and 2.1 at the lowest heights (excepting the coarsest soil TU-I where ER was 0.8), and lower than 1 at the greatest heights in most soils. At lower heights, both ER and the contents of fine sand tended to decrease from fine to sandy textured soils (Table 2). The ER for medium and coarse sand showed similar tendencies to fine sand, but their values were mostly higher than 1 at all saltation heights.

ER values for SOC were higher than 1 in most cases, reaching a maximum value of 3.4 in the sediment trapped at the highest height of the finest textured soil EH-II. Only in the coarsest soil TU-I, was the ER for SOC lower than 1 in the sediments trapped at 0.05, 0.13 and 0.315 m-height. The ER for SOC in the PM10 frac-

Table 2
Soil organic carbon enrichment ratios (SOC-ER) and grain size distribution of the trapped sediments and the PM10 fraction of each soil.

Soil	Sample	SOC-ER	Grain size distribution (μm)					
			0–3.9	3.9–31	31–62.5	62.5–125	125–250	250–2000
			%					
TU-I	Bulk soil	1.0	1	4	6	29	40	21
	0.05 m	0.9	0	2	4	32	44	18
	0.17 m	0.7	0	0	7	35	39	18
	0.315 m	0.9	0	0	7	42	40	11
	0.48 m	1.4	0	0	5	52	41	2
	PM10	5.4	16	51	17	14	2	0
TU-II	Bulk soil	1.0	2	6	8	29	32	24
	0.05 m	1.2	2	10	6	33	43	7
	0.17 m	1.7	0	2	9	32	36	21
	0.315 m	2.3	2	7	11	37	34	10
	0.48 m	3.0	3	14	7	35	35	7
	PM10	5.3	20	72	3	3	2	0
EH-I	Bulk soil	1.0	3	10	13	33	32	9
	0.05 m	1.1	1	5	7	34	41	12
	0.17 m	1.0	0	3	18	40	28	11
	0.315 m	1.0	0	2	17	45	30	7
	0.48 m	1.8	0	2	16	45	31	6
	PM10	4.4	20	73	5	5	0	0
EH-II	Bulk soil	1.0	2	8	8	21	39	21
	0.05 m	1.6	2	8	8	31	35	15
	0.17 m	1.7	2	6	13	34	31	15
	0.315 m	2.9	2	5	27	55	11	0
	0.48 m	3.4	2	5	8	33	39	13
	PM10	4.2	22	74	2	1	0	0

TU-I: Typic Ustipsamment from site I; TU-II: Typic Ustipsamment from site II; EH-I: Entic Haplustoll from site I; EH-II: Entic Haplustoll from Site II; Bulk soil: particles with a diameter less than 2 mm; 0.05 m, 0.17 m, 0.315 m and 0.48 m: sediments trapped at 0.05, 0.17, 0.315 and 0.48 m-height; PM10: particles with a diameter mainly < 10 μm.

tion reached the highest values, with a tendency to increase from fine (4.2) to sandy soils (5.4).

3.2. Mineral- and organic soil composition

The summed infrared signal intensities at the WN 3969 and 3619 cm^{-1}, assigned to O—H stretching in clay minerals (Madejova and Komadel, 2001), in the bulk soils and the PM10 fraction, showed an increase from sandy to finer textured soils as well as with increasing sampling height (Fig. 1).

Nevertheless, O—H signals were statistically not different between soils, excepting TU-I that showed the lowest signal intensities. For each site, the O—H signals of samples collected at the greatest height and of the PM10 fraction were higher than those of the bulk soil, while signals of the lowest heights were similar to the bulk soil.

In contrast to the O—H signals, the signal intensities at WN 791 cm^{-1}, assigned to Si—O groups of quartz (van der Marel and Beutelspacher, 1976), decreased with increasing height and from coarse to fine textured soils (Fig. 1). The PM10 fraction showed the lowest Si—O signal intensities. The significantly higher signal levels of both TU-I and TU-II, reflected their higher sand content (Table 1) compared to EH-I and EH-II.

The signal intensities of aliphatic C—H groups of SOM tended to increase with height and from sandy to fine textured soils (Fig. 2), with the exception of TU-II, where the signals at all heights were significantly lower than in the bulk soil.

Soil TU-I showed, on samples trapped at 0.48 m-height, a signal intensity for C—H groups five times higher than on all the trapped sediments at the same height. On the other hand, signal intensities of C—H groups of the PM10 fraction were higher in the sandiest TU-I than in the other finer textured soils. The signals of C—H groups of the PM10 fraction of both TU-I and TU-II were higher (ER of 2.2 and 1.5, respectively) than in the bulk soils, however, these signals were lower in both EH-I and EH-II (ER for C—H of 1.8 and 0.8, respectively) compared to the bulk soils.

The signal intensities of both C═O and C═C groups tended to slightly increase with height and from finer- to sandier textured soils in all analyzed samples (Fig. 2). However, only the smaller signal intensities of the PM10 fraction in comparison to the bulk soils and all the trapped sediments (Fig. 2), were significant.

The C—H/C═O ratios of the wind-eroded sediments trapped at the lowest heights (0.05 and 0.17 m) showed similar values to those of the bulk soils. However, at the greatest heights (0.315 and 0.48 m) these ratios increased from sandy to fine textured soils. An exception to this general trend was found for the coarsest TU-I, showing ratios at 0.48 m-height almost 6 times higher than in the other trapped sediments. The C—H/C═O ratios of the PM10 fraction increased from fine textured EH-I to the sandiest textured TU-I.

The signal intensities at WN 1035 cm^{-1}, assigned to both C—O—C and C—O groups slightly increased from sandy to fine textured soils in all analyzed samples (Fig. 2). No significant differences between the sediments trapped at all heights and the bulk soils were detected. However, the PM10 fraction showed significantly higher signal intensities than both the bulk soil and the trapped sediments trapped.

3.3. Discriminant analysis between the granulometry, SOC content and its composition

Fig. 3 shows the score plot of the most relevant components 1 and 2 of the PLSR analysis, where the information of the granulometric distribution and both the content and composition of SOC of the bulk soils, the trapped sediments and the PM10 fractions is summarized.

Component 1 was based on high absolute loading values between WN 3700 and 3000, 2000 and 1700, 1550 and 1250, and around 1100, 950, 750, and 600 cm^{-1}. Most of these spectral ranges were assigned to mineral functional groups as Si-O or groups related to texture as O—H, i.e., water adsorption in the clay fraction and/or clay minerals and quartz particles (Table A-1). The most important spectral differences belong to component 1

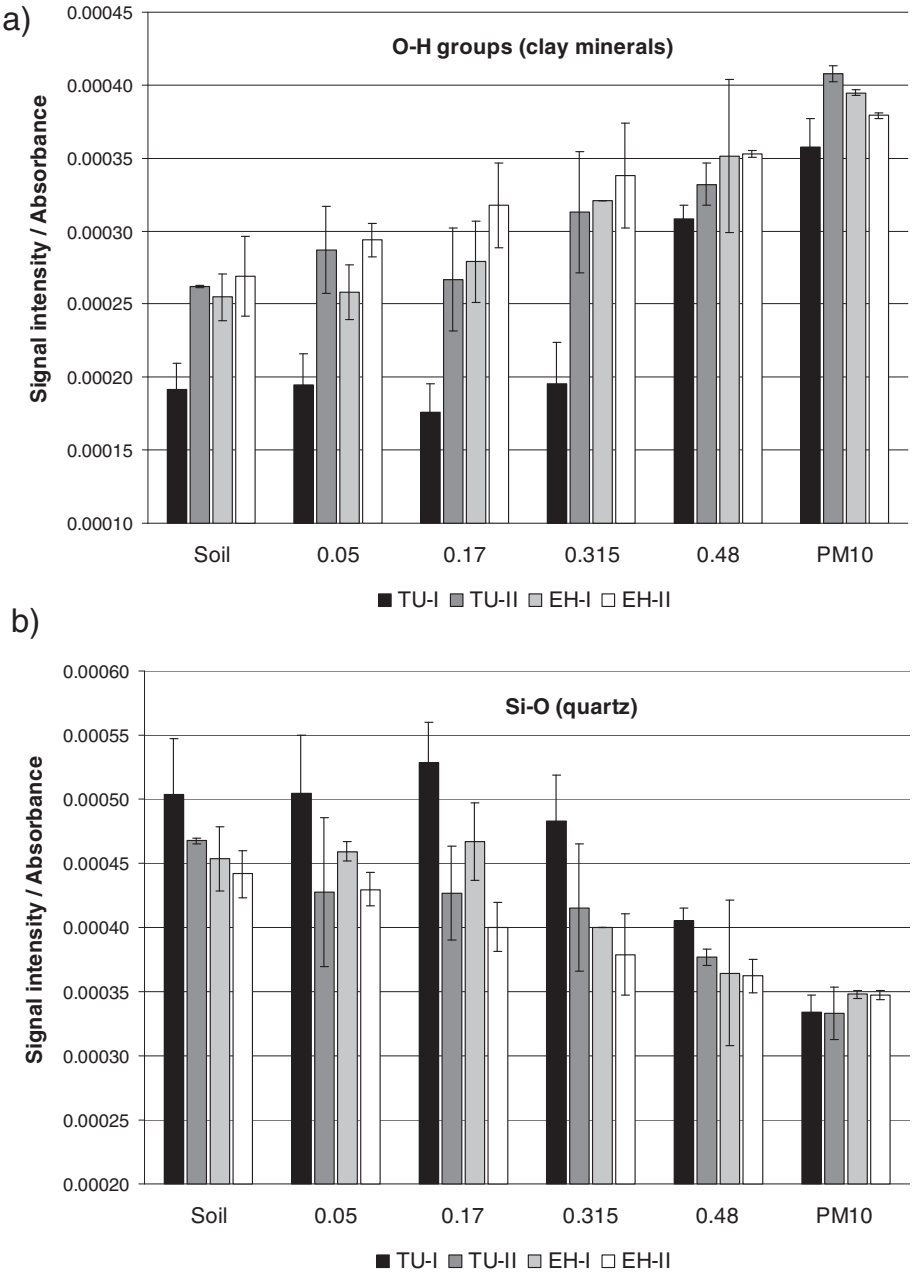

Fig. 1. Summed signal intensities from a) O—H groups of clay minerals at WN 3969 and 3619 cm^{-1} and b) Si—O groups of quartz at WN 791 cm^{-1} of the bulk soil (particles with a diameter less than 2 mm), the sediments trapped at different heights (0.05, 0.17, 0.315 and 0.48 m-height) and the PM10 fraction (particles with a diameter mainly less than 10 μm) from the four studied soils. TU-I: Typic Ustipsamment from site I, TU-II: Typic Ustipsamment from site II, EH-I: Entic Haplustoll from site I and EH-II: Entic Haplustoll from Site II. All the data are mean values of the signal intensities from triplicate samples and normalized by the spectral area.

(x-axis) and show the effect of the texture with an increasing relative particle size from the coarse (left) to the finer (right) textured samples. Component 1 also revealed clear differences between the PM10 fractions and the bulk soils and trapped sediments as well as between the bulk soils and the trapped sediments of the coarsest textured soil (TU-I; heights of 0.05, 0.17 and 0.315 m; Fig. 3).

Component 2 was based on loading values between WN 4000 and 3700, 3000 and 2400 and around 700 cm^{-1}. The region between WN 3000 and 2800 cm^{-1} is assigned to aliphatic C—H groups and the region around 700 cm^{-1} is assigned to Si—O stretching of both silicates and clay minerals (Table A-1). However, the influence of the other regions remains unclear. Note that indirect effects from both the broad O—H band of free water and from small baseline shifts, were corrected. Hence, as SOC content increase along the *y*-axis, the studied samples were mainly ordered according to their mineral composition, as was mentioned before, and secondly from lower to higher SOC content of the soils (Fig. 3 and Table 2). Highlighted differences according to SOC are shown for the sediment trapped at the greatest height (0.48 m) of the TU-I (Figs. 2 and 3), due to its high proportion of C—H-rich organic groups. The PM10 fractions of the four studied soils were characterized by the finest sized particles, clay and very fine silt, and the highest SOC contents. The PM10 fractions of fine soils EH-I and II, were dominated by their granulometric composition, which agreed with the negative correlation between clay and silt contents in the bulk soils and the SOC contents in the PM10 fraction ($r = 0.88$, $n = 4$). The PM10 of sandy soils, TU-I and TU-II, are more linked to SOM contents, indicating a mixture of low density labile organic particles.

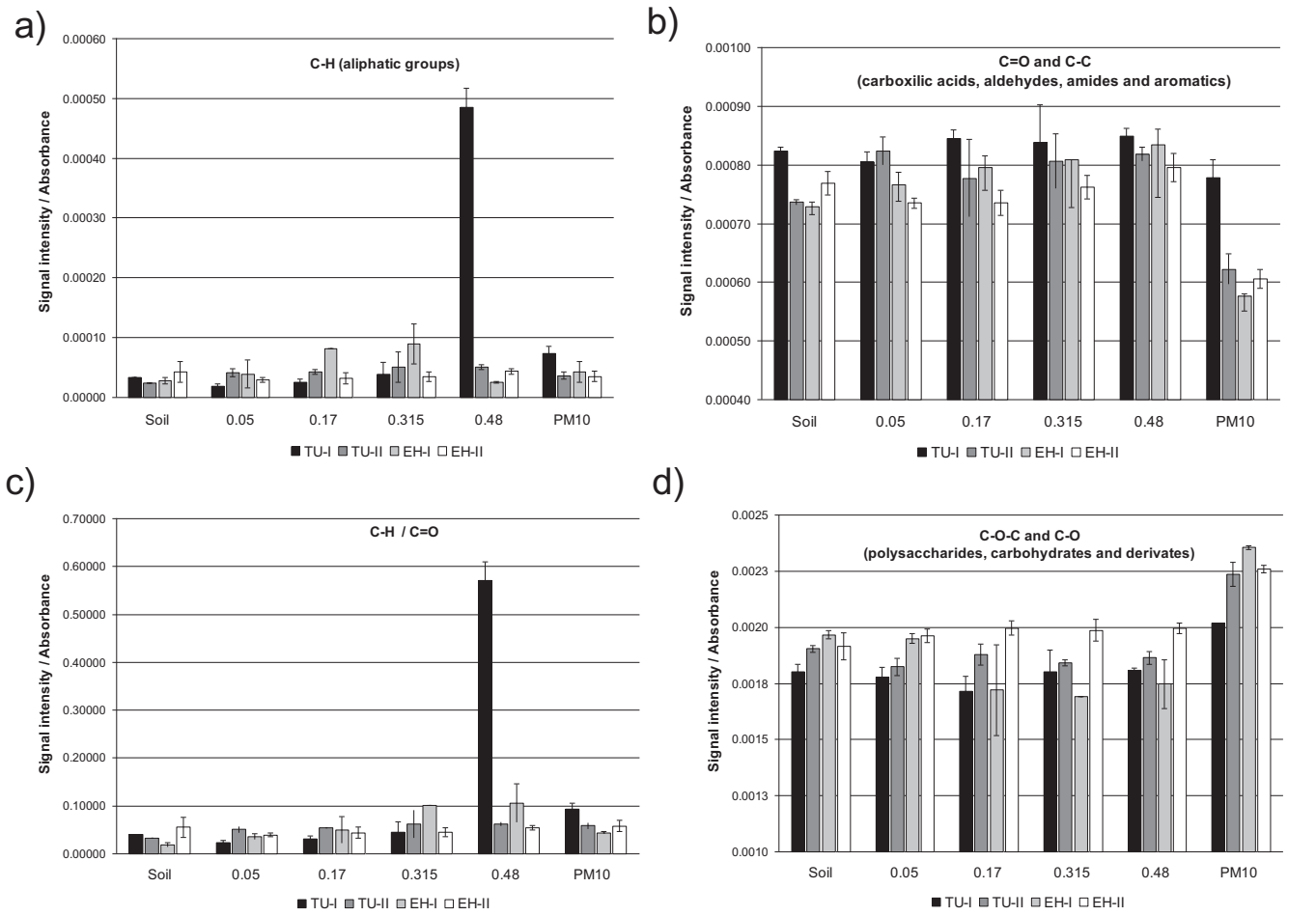

Fig. 2. Summed signal intensities from a) aliphatic C—H groups at WN 2962, 2924 and 2854 cm^{-1} and b) C=O and C=C groups at WN 1709, 1631 and 1611 cm^{-1}; c) C—H/C=O ratios of the soil organic matter and d) signal intensities of C—O—C groups of polysaccharides WN 1035 cm^{-1}, of the bulk soil (particles with a diameter less than 2 mm), the sediments trapped at different heights (0.05, 0.17, 0.315 and 0.48 m-height) and the PM10 fraction (particles with a diameter mainly less than 10 μm) from the four studied soils. TU-I: Typic Ustipsamment from site I, TU-II: Typic Ustipsamment from site II, EH-I: Entic Haplustoll from site I and EH-II: Entic Haplustoll from Site II. All the data are mean values of the signal intensities from triplicate samples and normalized by the spectral area.

4. Discussion

The increase in the proportion of fine sized particles (clay, silt and fine sand) with height in the eroded sediments of all studied soils is directly related to the relatively low weight and low settling velocities of these fractions, which are mixed by the turbulent wind transport into greater heights more easily. Similar findings have been previously presented by many other authors (e.g. Hoffmann et al., 2008; Kok et al., 2012; Sweeney and Mason, 2013).

The increase with height of the summed infrared signals of O—H functional groups corresponding to clay minerals and the decrease of the signal intensities of Si—O groups, linked with the presence of quartz, are consistent with the variations in the textural composition of the eroded sediments. The smaller contents of quartz grains, which have a greater density than clay aggregates, at the lowest sampling heights, and the higher contents of clays at greater heights correspond with the earlier results of Funk and Reuter (2006).

The proportion of clay and silt in the fine textured EH-I and EH-II was 3% higher at 0.48 m than at 0.05 m-height, while in the sandy soils TU-I and TU-II, this difference was even higher, reaching 8%. This tendency was more pronounced in the PM10 fraction, in which the proportion of clay and silt was 4.4 times higher than in the sediments trapped at 0.05 m in the finer soils EH-I and EH-II, while in the coarse textured soils TU-I and TU-II, this difference was even higher (8.5 times). Considering that, the saltation material of sandy soils is composed mainly of sand particles while that of fine textured soils, of clay- and silt aggregates (Avecilla et al., 2015), the results can be explained by the transport of silt and clay in aggregates at lower heights in fine textured soils. Therefore, the difference in clay and silt content between the sampling heights was lower than in sandy soils, in which most of the material transported close to the ground was composed by sand. Hence, sandy soils seem to be more affected by sorting processes than loamy soils.

In the PM10 fraction of the fine soils, between 2.1% and 16.8% particles with a diameter >30 μm (Table 2) were found, reaching 33% in the TU-I. Despite the electrostatic bonding force decreasing as particle-size increases (Peinemann et al., 2000), the silt fraction with diameters between 2 and 50 μm contribute 17% of the cation exchange capacity of these soils (Iturri and Buschiazzo, 2014). Therefore, not only were the aerodynamic properties a conditioning factor for the size of the material collected using the dust generator but the electrostatic properties of each soil were as well. For this reason, in this study the PM10 fraction was defined as the particulate matter with a diameter predominantly smaller than 10 μm.

The increasing SOC contents as sampling height increased can be related to the low density of the organic compounds that are mixed to greater heights. Many other authors (Buschiazzo and Funk, 2015; Chappell et al., 2014; Lal, 2003; Webb et al., 2012) have presented similar explanations for this observation. Other evidence of the transportation of low-density organic compounds at great height, was the presence of some large and loose organic

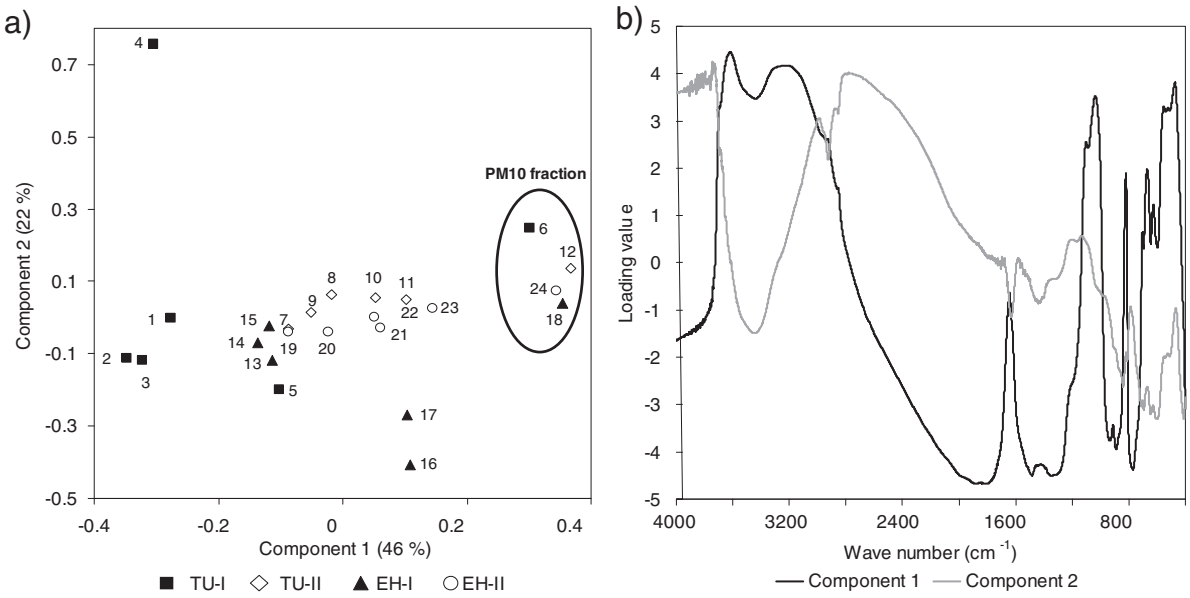

Fig. 3. a) Score plots and b) loadings of the components 1 and 2 most relevant for soil organic carbon (SOC) contents of the bulk soil (particles with a diameter less than 2 mm), the sediments trapped at different heights (0.05, 0.17, 0.315 and 0.48-m-height) and the PM10 fraction (particles with a diameter mainly less than 10 μm) from the four studied soils. TU-I: Typic Ustipsamment from site I, TU-II: Typic Ustipsamment from site II, EH-I: Entic Haplustoll from site I and EH-II: Entic Haplustoll from Site II. The numbers indicate: 1–6: bulk soil (1), sediments trapped at 0.05 (2), 0.17 (3), 0.315 (4) and 0.48 (5) m-height and the PM10 fraction (6) of the TU-I; 7–12: bulk soil (7), sediments trapped at 0.05 (8), 0.17 (9), 0.315 (10) and 0.48 (11) m-height and the PM10 fraction (12) of the TU-II; 13–18: bulk soil (13), sediments trapped at 0.05 (14), 0.17 (15), 0.315 (16) and 0.48 (17) m-height and the PM10 fraction (18) of the EH-I and, 19–24: bulk soil (19), sediments trapped at 0.05 (20), 0.17 (21), 0.315 (22) and 0.48 (23) m-height and the PM10 fraction (24) of the EH-II.

particles in the sediments trapped at 0.48 m-height. These particles correspond to plant debris that are mixed but not aggregated with mineral particles, particularly with sand particles in the coarser texture soils. The 0.48 m-height trapped sample of the TU-I was the most outstanding case because of its high amount of loose plant debris (Fig. 4), in consistency with its high signal intensity for C—H groups (Fig. 2). However, the organic compounds were detected as part of the aggregates in the PM10 fraction of the four studied soils. The scanning - laser microscope images of the PM10 fractions (Fig. 5) allowed their visualization.

The higher ER of SOC in the PM10 fraction of sandy soils (TU-I and TU-II) compared to those of fine textured soils (EH-I and EH-II), may be related to organic compounds, which are incorporated into large- and less erodible aggregates in finer soils (Buschiazzo and Taylor,1993; Aimar et al., 2012). Because of this, though sandy bulk soils contained lower amounts of SOC, their emitted PM10 fractions have relatively high amounts of SOC in the form of fine- and light aggregates or small pieces of plant and other organic debris.

As shown in Fig. 5, the ER of SOC of the trapped sediments in the wind tunnel are similar to those found by other authors for sediments collected at similar heights, under field conditions, and from soils alike in texture to the soils used in this study. The ER of SOC of the PM10 fractions are in the same range as those measured by other authors (Bach, 2008; Funk, 1995, 2004; Larney et al., 1998; Li et al., 2007; Mendez et al., 2011; Ramsperger et al., 1998; Sterk et al., 1996) in similar-sized wind eroded sediments collected at 4 m-height, under field conditions. In addition, due to the flattening of the curve, it can be interpreted that the ER values would not change with increasing height above 4 m. Thus, the ER of SOC of the PM10 fractions generated and collected by the laboratory method are similar to those measured on sediments released during wind erosion events. This allows us to confirm that the PM10 fraction artificially obtained in this study is representative of the PM10 emitted under natural conditions. Therefore, the dust generator (EDG, Mendez et al., 2013) used seems to be a reliable device to separate PM10 from bulk soils for analysis purposes.

The higher C=O and C=C signals for carboxylic acids, aldehydes, amides and aromatics (Baes and Bloom, 1989; Senesi et al., 2003; Demyan et al., 2012; Leue et al., 2015) at lower heights may be

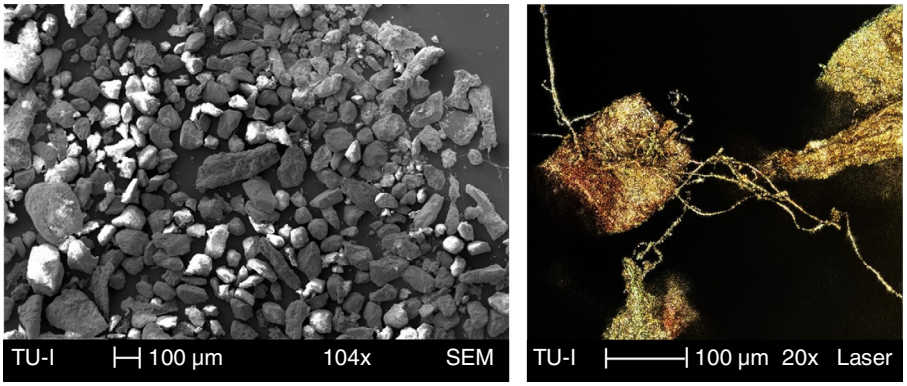

Fig. 4. Microscope images of the 0.48 m-height trapped sediment of the TU-I (Typic Ustipsamment from site I). Left-side figure shows a SEM 104× image and right-side figure, a color + laser 20× image, showing the mineral particles, dominated by sand, and plant debris, their arrangement and size.

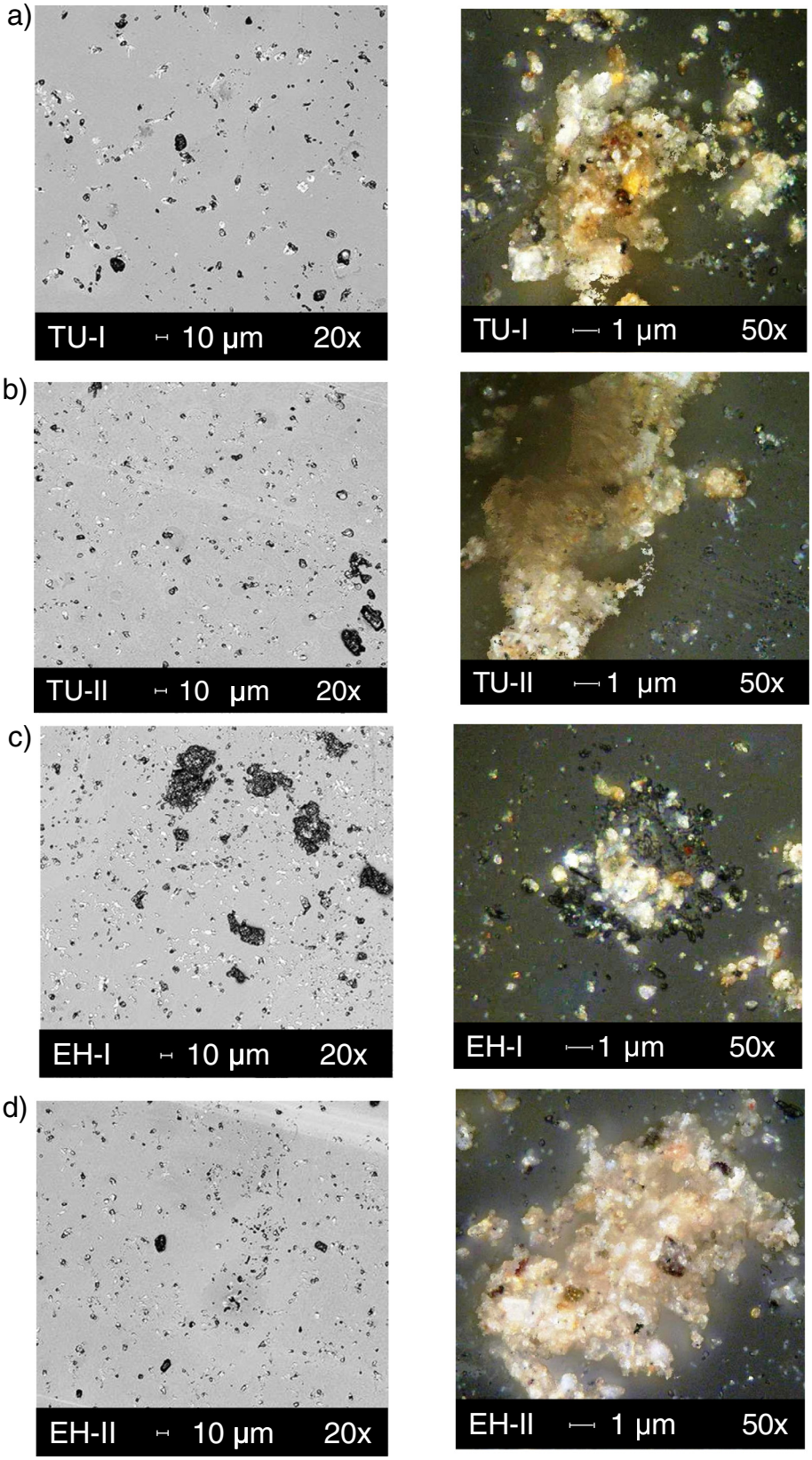

Fig. 5. Laser microscope images of the PM10 fraction from the a) TU-I (Typic Ustipsamment from site I), b) TU-II (Typic Ustipsamment from site II), c) EH-I (Entic Haplustoll from site I) and d) EH-II (Entic Haplustoll from Site II). For each soil, left-side figures show an overview of the dust samples mainly composed of particles <10 µm (laser, 20×) and right-side figures, a detailed view of the microaggregates in this fraction (color, 50×). Light-colored particles in the color, 50× images denote mineral particles while dark-colored are the organic particles.

due to increasing proportions of these intermediate- to stable organic compounds in coarse and relatively heavy aggregates. On the other hand, the increasing amounts of labile C—H groups from plant debris or incompletely decomposed SOM, indicate that light organic materials are transported to higher heights because of their low density (Balesdent et al., 2000).

The differences in the C—H/C=O ratios revealed that the SOC content and the SOM composition, between the sites and the different samples in height were different. The higher C—H/C=O ratios of the PM10 fractions compared to the bulk soils and the trapped sediments, indicate an enrichment of plant debris and microbial biomass in this fraction (Kalbitz et al., 2003; Conen and Leifeld, 2014; Conen et al., 2011). However, while the occurrence of plant debris seems to be limited by its size in the PM10 fraction, the assumption of increased proportions of microbial biomass is underlined by higher signal intensities of C—O—C and C—O groups in this fraction than in the trapped sediments and the bulk soils (Fig. 2). The microbial biomass compounds could act as aggregating agents in the finest pores of microaggregates of the PM10 fractions (Fig. 5), contributing to slower decomposition rates as compared to organic matter associated with larger aggregates (Elliot, 1986; Beare et al., 1994; Gupta and Germina, 1988; Jastrow et al., 1996).

The high proportion of aliphatic C—H groups found in the 0.48 m-height trapped sediment of TU-I (Fig. 2) can be explained by the small degree of aggregation of this sandy and SOC-poor soil (Table 1) (Buschiazzo and Taylor, 1993; Aimar et al., 2012). In TU-I, therefore, plant debris was not incorporated into aggregates (Fig. 4) and remained as particulate organic matter (POM) (Six et al., 2004). Moreover, due to its lower density, POM would have been easily transported by WE to greater heights (Buschiazzo and Funk, 2015; Lal, 2003) although, due to its large size it would not be included in the PM10 fraction. The occurrence of high POM amounts in the TU-I could be caused by the recent use of the soil as grasslands (Noellemeyer et al., 2008; Zach et al., 2006), i.e., these soil was out of cultivation for some time.

According to the differences in the SOM composition, the PM10 fraction from the TU-I site should reveal different physico-chemical properties, e.g., a higher water repellency (Leue et al., 2015), as result of higher C—H proportions, compared to the PM10 fraction release from the TU-II, EH-I and EH-II.

5. Conclusions

- Due to sorting by wind, sandy soils yield more eroded sand at lower heights while finer soils have higher silt and clay contents at lower heights.
- SOC content increased with sampling height in all studied soils. This was due to the transport of low density compounds (plant debris and SOC of microbial origin) to greater heights, and coarse aggregates compounds (carboxylic acids, aldehydes, amides and aromatics) remaining at low heights.
- The SOC content of the PM10 fractions was higher in sandy than in fine textured soils.
- Sandy soils lead to a more intensive separation of organic and mineral particles as height increases compared to fine textured soils. Thus, the coarse textural fractions and organic matter compounds transported by saltation could result in nutrient losses and their deposition in adjacent ecosystems. However, due to the mobility and composition of the PM10 fraction emitted from agricultural soils, it could influence processes like C sequestration or cloud formation at the regional or global scale.

Acknowledgements

This study was supported by the joint project "Multiscale analysis of quantitative and qualitative fine particulate matter emissions from agricultural soils of La Pampa, Argentina" funded by the Ministry for Science, Technology and Innovative Production of Argentina (MINCyT), the National Council for Research and Technology of Argentina (CONICET) and the Deutsche Forschungsgemeinschaft (DFG) of Germany FU247/10-1, as well as by the PICT 2011N° 354-, the PIP 2011–2013/CONICET 111 201101 00017- and the DFG LE 3177/1-1 projects.

Authors wish to thank Dr. F. Avecilla and J.E. Panebianco for performing the wind tunnel simulations and Biol. J. Busse for performing the SEM observations.

Appendix A

Table A-1
Wave number positions, assignments of mineral and/or organic functional groups and literature references of analyzed infrared signal intensities.

Wave number cm^{-1}	Functional group	Band assignment	Reference
3696, 3619	O—H	O—H stretching of structural hydroxyls of clay minerals	van der Marel and Beutelspacher (1976), Madejova and Komadel (2001)
3435	O—H	O—H stretching in free water and in intermolecular hydrogen bonds of SOM (hydroxyls, phenols, saccharides, soil minerals)	Stevenson (1994), Senesi et al. (2003)
2956, 2925, 2859	C—H aliphatic	C—H asymmetric stretching in alkyl CH_3 and CH_2; C—H symmetric stretching in alkyl CH_2	Baes and Bloom (1989), Capriel et al. (1995), Capriel (1997)
1709	C=O	C=O stretching in saturated and unsaturated fatty acids, ketones	
1630	C=O	C=O stretching of carboxylate in mono- and di-substituted amides	Senesi et al. (2003), Baes and Bloom (1989), Stevenson (1994)
	C=C	C=C stretching of carboxylate ions; C=C conjugated with aromatic ring	
	N—H	N—H bending of NH_2 in primary amides	
1611	C=O	C=O stretching in carboxylate ions; C=C stretching in aromatics	Bornemann et al. (2008)
	C=C		
1380	C=O	C=O symmetric stretching in carboxylate ions	Hesse et al. (1984), Senesi et al. (2003), Spence and Kelleher (2012)
1085	Si—O—Si	Si—O—Si stretching in silicates	Senesi et al. (2003)
	C—O	R_3C—OH stretching in alcohols and phenols	
		C—O—H bending	
1034	Si—O—Si	Si—O—Si stretching in silicates and clay minerals	Hesse et al. (1984), Senesi et al. (2003)
	O—Al—OH	O—Al—OH stretching in clay minerals	
	C—O—C	C—O—C stretching in polysaccharides/carbohydrates (derivatives)	
	C—O	C—O stretching in alcohols	
780	Si—O	Si—O stretching of silicates	Madejova and Komadel (2001)

References

Aimar, S.B., 2002. Estimaciones cualitativas y cuantitativas de pérdidas por erosión eólica en suelos dela región semiárida pampeana central. UNS, Bahía Blanca.

Aimar, S.B., Buschiazzo, D.E., Peinemann, N., 2002. Pérdidas de materia orgánica y elementos en suelos de la región semiárida Argentina, producidos por erosión eólica, XVIII Congreso Argentino de la Ciencia del Suelo, Puerto Madryn.

Aimar, S.B., Mendez, M.J., Funk, R., Buschiazzo, D.E., 2012. Soil properties related to potential particulate matter emissions (PM10) of sandy soils. Aeolian Res. 3, 437–443.

Ajwa, H.A., Sullivan, D.A., 2011. Evaluation of wind erosion emissions factors for air quality modeling. Soil Sci. Soc. Am. J. 75, 1285–1294.

Avecilla, F., Panebianco, J.E., Buschiazzo, D.E., 2015. Variable effects of saltation and soil properties on wind erosion of different textured soils. Aeolian Res. 18, 145–153.

Bach, M., 2008. Aolische Stofftransporte in Agrarlandschaften (PhD Dissertation). Christian- Albrechts Universitat, Kiel.

Baes, A.U., Bloom, P.R., 1989. Diffuse reflectance and transmission Fourier transform infrared (DRIFT) spectroscopy of humic and fulvic acids. Soil Sci. Soc. Am. J. 53, 695–700.

Balesdent, J., Chenu, C., Balabane, M., 2000. Relationship of soil organic matter dynamics to physical protection and tillage. Soil Tillage Res. 53, 215–230.

Beare, M.H., Cabrera, M.L., Hendrix, P.F., Coleman, D.C., 1994. Aggregate-protected and unprotected organic matter pools in conventional- and no-tillage soils. Soil Sci. Soc. Am. J. 58, 787–795.

Bornemann, L., Welp, G., Brodowsky, S., Rodionow, A., Amelung, W., 2008. Rapid assessment of black carbon in soil organic matter using mid-infrared spectroscopy. Org. Geochem. 39, 1537–1544.

Buschiazzo, D.E., Funk, R., 2015. Wind erosion of agricultural soils and the carbon cycle. In: Banwart, S.A., Noellemeyer, E.J., Milne, E. (Eds.), Soil Carbon Science, Management and Policy for Multiple Benefits. CAB International, Wallingford, pp. 161–168.

Buschiazzo, D.E., Taylor, V., 1993. Efectos de la erosion eolica sobre algunas propiedades de suelos de la region Semiarida Pampeana Argentina. Ciencia del Suelo 10, 46–53.

Buschiazzo, D.E., Panigatti, J.L., Unger, P.W., 1998. Tillage effects on soil properties and crop production in the subhumid and semiarid Argentinean Pampas. Soil Tillage Res. 49, 105–116.

Capriel, P., 1997. Hydrophobicity of organic matter in arable soils: influence of management. Eur. J. Soil Sci. 48, 457–462.

Capriel, P., Beck, T., Borchert, H., Gronholz, J., Zachmann, G., 1995. Hydrophobicity of the organic matter in arable soils. Soil Biol. Biochem. 27, 1453–1458.

Chappell, A., 2016. Wind erosion reduces soil organic carbon sequestration falsely indicating ineffective management practices. Aeolian Res. 22, 107–116.

Chappell, A., Webb, N.P., Viscarra Rossel, R.A., Bui, E., 2014. Australian net (1950s–1990) soil organic carbon erosion: implications for CO2 emission and land-atmosphere modelling. Biogeosciences 11, 5235–5244.

Conen, F., Leifeld, J., 2014. A new facet of soil organic matter. Agric. Ecosyst. Environ. 185, 186–187.

Conen, F., Morris, C.E., Leifeld, J., Yakutin, M.V., Alewell, C., 2011. Biological residues define the ice nucleation properties of soil dust. Atmos. Chem. Phys. 11, 9643–9648.

Demyan, M.S., Rasche, F., Schulz, E., Breulmann, M., Müller, T., Cadisch, G., 2012. Use of specific peaks obtained by diffuse reflectance Fourier transform mid-infrared spectroscopy to study the composition of organic matter in a Haplic Chernozem. Eur. J. Soil Sci. 63, 189–199.

Dockery, D.W., Pope, C.A., Xu, X., Spengler, J.D., Ware, J.H., Fay, M.E., Ferris, B.G., Speizer, F.E., 1993. An association between air pollution and mortality in six U.S. cities. N. Engl. J. Med. 329, 1753–1759.

Dong, Z.B., Chen, G.T., 1997. A preliminary insight in to the wind erosion problem in Houshan area of Inner Mongolia. J. Soil Water Conserv. 3, 84–90.

Elliot, E.T., 1986. Aggregate structure and carbon, nitrogen and phosphorus in native and cultivated soils. Soil Sci. Soc. Am. J. 50, 627–633.

Fröhlich-Nowoisky, J., Burrows, S.M., Xie, Z., Engling, G., Solomon, P.A., Fraser, M.P., Mayol-Bracero, O.L., Artaxo, P., Begerow, D., Conrad, R., Andreae, M.O., Després, V.R., Pöschl, U., 2012. Biogeography in the air: fungal diversity over land and oceans. Biogeosciences 9, 1125–1136.

Fryrear, D.W., Saleh, A., Bilbro, J.D., Schomberg, H.M., Stout, J.E., Zobeck, T.M., 1998. Revised Wind Erosion Equation (RWEQ). Wind erosion and water conservation research unit: Technical Bulletin N° 1. USDA-ARS, Southern Plains Area Cropping Systems Research Laboratory, Big Spring.

Funk, R., 1995. Quantifizierung der Winderosion auf einem Sandstandort unter besonderer Berücksichtigung der Vegetationswrikung. ZALF-Bericht, Müncheberg.

Funk, R., 2004. Viel Wind um Nichts? Forschungen zur Winderosion in Brandemburg. Arch. Agron. Soil Sci. 50, 309–317.

Funk, R., Reuter, H.I., 2006. Wind erosion. In: Boardman, J., Poesen, J. (Eds.), Soil Erosion in Europe. John Wiley & Sons, Chichester, pp. 553–582.

Gaiero, D.M., Depetris, P.J., Probst, J.L., Bidart, S.M., Leleyter, L., 2004. The signature of river- and wind-borne materials exported from Patagonia to the southern latitudes: A view from REEs and implications for paleoclimatic interpretations. Earth Planet. Sci. Lett. 219, 357–376.

Goossens, D., Gross, J., 2002. Similarities and dissimilarities between the dynamics of sand and dust during wind erosion of loamy sandy soil. Catena 47, 269–289.

Gupta, V.V.S.R., Germina, J.J., 1988. Distribution of microbial biomass and its activity in different soil aggregate size classes affected by cultivation. Soil Biol. Biochem. 20, 777–786.

Harrison, R.M., Deacon, A.R., Jones, M.R., Appleby, R.S., 1997. Sources and processes affection concentrations of PM10 and PM2.5 particulate matter in Birmingham (U.K.). Atmos. Environ. 31, 4103–4117.

Hesse, M., Meier, H., Zeeh, B., 1984. Spectrocopic Methods in Organic Chemistry. Georg Thieme, Stuttgart.

Hoffmann, C., Funk, R., Sommer, M., Li, Y., 2008. Temporal variations in PM10 and particle size distribution during Asian dust storms in Inner Mongolia. Atmos. Environ. 42, 8422–8431.

Hoffmann, C., Funk, R., Reiche, M., Li, Y., 2011. Assessment of extreme wind erosion and its impacts in Inner Mongolia, China. Aeolian Res. 3, 343–351.

Iturri, L.A., Buschiazzo, D.E., 2014. Mineralogy and cation exchange capacity of size fractions of a loess soil climosequence. Catena 121, 81–87.

Jastrow, J.D., Boutton, T.W., Miller, R.M., 1996. Carbon dynamics of aggregate-associated organic matter estimated by carbon-13 natural abundance. Soil Sci. Soc. Am. J. 60, 801–807.

Kalbitz, K., Schwesig, D., Schmerwitz, J., Kaiser, K., Haumanier, L., Glaser, B., Ellerbrock, R., Leinweber, P., 2003. Changes in properties of soil-derived dissolved organic matter induced by biodegradation. Soil Biol. Biochem. 35, 1129–1142.

Kok, J.F., Parteli, E.J.R., Michaels, T.I., Karam, D.B., 2012. The physics of wind-blown sand and dust. Rep. Prog. Phys. 75, 106–109.

Lal, R., 2003. Soil erosion and the global carbon budget. Environ. Int. 29, 437–450.

Larney, F.J., Bullock, M.S., Janzen, H.H., Ellert, B.H., Olson, E.C.S., 1998. Wind erosion effects on nutrient redistribution and soil productivity. J. Soil Water Conserv. 53, 133–140.

Lenes, J.M., Prospero, J.M., Landing, W.M., Virmani, J.I., Walsh, J.J., 2012. A model of Saharan dust deposition to the eastern Gulf of Mexico. Mar. Chem. 134, 1–9.

Leue, M., Gerke, H.H., Godow, S.C., 2015. Droplet infiltration and organic matter composition of intact crack and biopore surfaces from clay-illuvial horizons. J. Plant Nutr. Soil Sci. 178, 250–260.

Li, J., Okin, G.S., Alvarez, L., Epstein, H., 2007. Quantitative effects of vegetation cover on wind erosion and soil nutrient loss in a desert grassland of southern New Mexico, USA. Biogeochemistry 85, 317–332.

Madejova, J., Komadel, P., 2001. Baseline studies of the clay minerals society source clays: infrared methods. Clay. Clay Miner. 49, 410–432.

Martin, J.H., Gordon, R.M., Fitzwater, S.E., 1991. The case for iron. Limnol. Oceanogr. 36, 1793–1802.

Mc Lean, E.O., 1982. Soil pH and lime requirement. In: Page, A.L., Miller, R.H., Keeney, D.R. (Eds.). . second ed., Methods of Soil Analysis. Part 2-Chemical and Microbiological Properties second ed., vol. 1 SSSA, Madison, pp. 199–223.

Mendez, M.J., Funk, R., Buschiazzo, D.E., 2011. Efficiency of big spring number eight (BSNE) and modified Wilson and Cook (MWAC) samplers to collect PM10, PM2.5 and PM1. Aeolian Res. 21, 37–44.

Mendez, M.J., Panebianco, J.E., Buschiazzo, D.E., 2013. A new dust generator for laboratory dust emission studies. Aeolian Res. 8, 59–64.

Michelena, R., Irurtia, C., 1995. Susceptibility of soil to wind erosion in La Pampa province. Arid Soil Res. Rehabil. J. 9, 227–234.

Morman, S.A., Plumlee, G.S., 2013. The role of airborne mineral dusts in human disease. Aeolian Res. 9, 203–212.

Nerger, R., Funk, R., Cordsen, E., Fohrer, N., 2017. Application of a modeling approach to designate soil and soil organic carbon loss to wind erosion on long-term monitoring sites (BDF) in Northern Germany. Aeolian Res. 25, 135–147.

Noellemeyer, E., Frank, F., Alvarez, C., Morazzo, G., Quiroga, A., 2008. Carbon contents and aggregation related to soil physical and biological properties under a land-use sequence in the semiarid region of central Argentina. Soil Tillage Res. 99, 179–190.

Nordstrom, K.F., Hotta, S., 2004. Wind erosion from cropland in the USA: a review of problems, solutions and prospects. Geoderma 121, 157–167.

Panebianco, J.E., Mendez, M.J., Buschiazzo, D.E., 2016. PM10 emission, sandblasting efficiency and vertical entrainment during successive wind-erosion events: a wind-tunnel approach. Boundary-Layer Meteorol. 161, 335–353.

Peinemann, N., Amiotti, N.M., Zalba, P., Villamil, M.B., 2000. Minerales de arcilla en fracciones limo de horizontes superficiales de suelos de diferente mineralogía. Ciencia del Suelo 18, 69–72.

Pope III, C.A., Dockery, D.W., 2006. Health effects of fine particulate air pollution: lines that connect. J. Air Waste Manage. Assoc. 56, 709–742.

R Core Team, 2014. A language and environment for statisticalcomputing. R Foundation for Statistical Computing, Vienna. <http://www.R-project.org/>.

Ramsperger, B., Peinemann, N., Stahr, K., 1998. Deposition rates and characteristics of aeolian dust in the semi-arid and sub-humid regions of the Argentinean Pampa. J. Arid Environ. 39, 467–476.

Ravi, S., D'Odorico, P., Breshears, D.D., Field, J.P., Goudie, A.S., Huxman, T.E., Li, J., Okin, G.S., Swap, R.J., Thomas, A.D., Van Pelt, S., Whicker, J.J., Zobeck, T.M., 2011. Aeolian processes and the biosphere. Rev. Geophys. 49, 1–45.

Roney, J.A., White, B.R., 2006. Estimating fugitive dust emission rates using an environmental boundary layer wind tunnel. Atmos. Environ. 40, 7668–7685.

Schäfer, P., Reiss, C., Albrecht, P., 1995. Geochemical study of macromolecular organic matter from sulfur-rich sediments of evaporitic origin (Messinian of Sicily) by chemical degradations. Org. Geochem. 23, 567–581.

Senesi, N., D'Orazio, V., Ricca, G., 2003. Humic acids in the first generation of Eurosoils. Geoderma 116, 325–344.

Shao, Y., Wyrwoll, K.H., Chappell, A., Huang, J., Lin, Z., McTainsh, G.H., Mikami, M., Tanaka, T.Y., Wang, X., Yoon, S., 2011. Dust cycle: an emerging core theme in Earth system science. Aeolian Res. 2, 181–204.
Sharratt, B.S., Graves, L., Pressley, S., 2015. Nitrogen loss from windblown agricultural soils in the Columbia Plateau. Aeolian Res. 18, 47–53.
Six, J., Bossuyt, H., Degryze, S., Denef, K., 2004. A history of research on the link between (micro) aggregates, soil biota, and soil organic matter dynamics. Soil Tillage Res. 79, 7–31.
Soil Survey Staff, 1999. Soil Taxonomy: A Basic System of Soil Classification for Making and Interpreting Soil Surveys. U.S. Government Printing Office, Washington.
Spence, A., Kelleher, B.P., 2012. FT-IR spectroscopic analysis of kaolinite-microbial interactions. Vib. Spectrosc. 61, 151–155.
Steinke, I., Funk, R., Busse, J., Iturri, A., Kirchen, S., Leue, M., Möhler, O., Schwartz, T., Schnaiter, M., Sierau, B., Toprak, E., Ullrich, R., Ulrich, A., Hoose, C., Leisner, T., 2016. Ice nucleation activity of agricultural soil dust aerosols from Mongolia, Argentina and Germany. J. Geophys. Res. Atmos. 121, 13559–13576.
Sterk, G., Herrmann, L., Bationo, A., 1996. Wind-blown nutrient transport and soil productivity changes in the southwest Niger. Land Degrad. Dev. 7, 325–335.
Stevenson, F.J., 1994. Humus Chemistry: Genesis, Composition, Reactions. John Wiley & Sons, New York.
Sweeney, M.R., Mason, J.A., 2013. Mechanisms of dust emission from Pleistocene loess deposits, Nebraska, USA. J. Geophys. Res. Earth Surf. 118, 1460–1471.
Tan, S.C., Shi, G.Y., Shi, J.H., Gao, H.W., Yao, X., 2011. Correlation of Asian dust with chlorophyll and primary productivity in the coastal seas of China during the period from 1998 to 2008. J. Geophys. Res. Biogeosci. 116, 1–10.
Tanaka, T.Y., Chiba, M., 2006. A numerical study of the contributions of dust source regions to the global dust budget. Global Planet. Change 52, 88–104.
Van der Marel, H.W., Beutelspacher, H., 1976. Atlas of Infrared Spectroscopy of Clay Minerals and Their Admixtures. Elsevier, Amsterdam.
Webb, N.P., Chappell, A., Strong, C.L., Marx, S.K., McTainsh, G.H., 2012. The significance of carbon-enriched dust for global carbon accounting. Global Change Biol. 18, 3275–3278.
Webb, N.P., Herrick, J.E., Van Zee, J.W., Courtright, E.M., Hugenholtz, C.H., Zobeck, T. M., Okin, G.S., Barchyn, T.E., Billings, B.J., Boyd, R., Clingan, S.D., Cooper, B.F., Duniway, M.C., Derner, J.D., Fox, F.A., Havstad, K.M., Heilman, P., LaPlante, V., Ludwig, N.A., Metz, L.J., Nearing, M.A., Norfleet, M.L., Pierson, F.B., Sanderson, M. A., Sharratt, B.S., Steiner, J.L., Tatarko, J., Tedela, N.H., Toledo, D., Unnasch, R.S., Van Pelt, R.S., Wagner, L., 2016. The National Wind Erosion Research Network: building a standardized long-term data resource for aeolian research, modeling and land management. Aeolian Res. 22, 23–36.
Wentworth, C.K., 1922. A scale of grade and class terms for clastic sediments. J. Geol. 30, 377–392.
Yan, H., Wang, S., Wang, C., Zhang, G., Patel, N., 2005. Losses of soil organic carbon under wind erosion in China. Global Change Biol. 11, 828–840.
Zach, A., Tiessen, H., Noellemeyer, E., 2006. Carbon turnover and carbon-13 natural abundance under land use change in semiarid savanna soils of La Pampa, Argentina. Soil Sci. Soc. Am. J. 70, 154–161.
Zobeck, T.M., Baddock, M., Scott Van Pelt, R., Tatarko, J., Acosta-Martinez, V., 2013. Soil property effects on wind erosion of organic soils. Aeolian Res. 10, 43–51.